



Research paper

Ferrocene appended fluorescein-based ratiometric fluorescence and electrochemical chemosensor for Fe³⁺ and Hg²⁺ ions in aqueous media: Application in real samples analysis

Sushil Ranjan Bhatta^a, Adwitiya Pal^a, Ujwal K. Sarangi^b, Arunabha Thakur^{a,*}^a Department of Chemistry, Jadavpur University, Kolkata 700032, India^b Department of Chemistry, Vikram Deb (auto) College, Jeypore, Odisha 764001, India

ARTICLE INFO

Keywords:

Ferrocene
Ratiometric fluorescence
Electrochemistry
Fluorescein
Click chemistry

ABSTRACT

A novel visually detectable fluorescein-based chemosensor (**4**) containing a ferrocene backbone has been designed and synthesized successfully by simultaneously introducing ferrocene with an azide appendage and fluorescein with an alkyne functional group via a [2 + 3] cycloaddition reaction. Further, its sensing response towards various metal cations was examined via multiple channels. The probe shows a remarkable specificity towards Fe³⁺ and Hg²⁺ ions through “naked-eye” detection as well as via ratiometric fluorescence emission with limits of detection of 9.75×10^{-8} M and 39×10^{-8} M for Fe³⁺ and Hg²⁺ ions, respectively. Further, shifts in the voltammogram towards anodic potential of $\Delta E_{1/2} = 31$ and 33 mV are observed upon binding Fe³⁺ and Hg²⁺ ions, respectively. Characterization of compound **4** has been done by ¹H NMR, ¹³C NMR, high-resolution mass spectrometry (HRMS) and CHN analysis studies. The stoichiometry of the complex of the present probe with either Fe³⁺ or Hg²⁺ is indicative of a 1:1 ratio, which was determined by Job's plot as well as ¹H NMR titration data. The incorporation of compound **4** in solid support has made the work more practicable. In addition, the practical application of receptor **4** was successfully explored towards the detection of Fe³⁺ and Hg²⁺ ions in real water samples by using the different water sources.

1. Introduction

Molecular fluorescence detection, among the various detection techniques possible, is a well-grounded method for the analysis of a variety of biological events [1–3]. However, fluorescence “turn-off” or “turn-on” responses where the measurement is based on the single signal (the change of fluorescence intensity) encountered many drawbacks such as limitations with respect to excitation intensity, probe concentrations, and instrumental efficiency etc. [4,5]. Further advancement in this field has led to ratiometric fluorescence studies, which utilize the ratio of the emission intensity at two different wavelengths, and are always advantageous as they can overcome the above-mentioned problems to make the results precise and accurate [6,7]. Ratiometric fluorescence sensing, among all other optical sensing methods currently being explored, has received particular attention as a technique with the potential to provide precise and quantitative analyses with high sensitivity and inherent reliability [8,9]. In our work, we have chosen fluorescein as our basic fluorophore unit. This interest stems from its manifold advantages, such as its favorable photophysical

properties [10], high absorption coefficient, excitation and emission wavelengths in the visible region with a high fluorescence quantum yield and high photostability [11–14], easy synthesis and functionalization [15], excellent biocompatibility and cellular membrane-penetrating capacity [16]. It is a widely used fluorescent probe in biosciences [17–20] for the lipophilic properties of its alkyl, ester and ether derivatives [21]. On the other hand, the wide chemical functionality of ferrocene and its derivatives has resulted in their use as extra-ordinarily robust building blocks for the preparation of multi-responsive chemosensors. They have been considered as prototype chemosensors owing to their interesting electrochemical and optical sensing properties [22]. Therefore, the combination of these two moieties, in principle, should develop a potential molecular system for the detection of toxic metal ions.

Detection of a toxic metal ion that influences the physiological and pathological processes in living systems [23] has attracted great interest around the globe and is considered one of the forefront research areas in supramolecular chemistry. Fluorescence chemosensors, especially ratiometric fluorescence chemosensors, prone to give precise and

* Corresponding author.

E-mail address: arunabha.thakur@jadavpuruniversity.in (A. Thakur).<https://doi.org/10.1016/j.ica.2019.119097>

Received 19 June 2019; Received in revised form 26 August 2019; Accepted 26 August 2019

Available online 27 August 2019

0020-1693/ © 2019 Elsevier B.V. All rights reserved.

quantitative optical output by addition of proper analyte (e.g. metal ions, anions or biologically relevant small molecules), have come to prior action [24]. The extension to a real time procedure owing to its sensitive responses, instrumentation viability, economically affordable nature and profuse biocompatibility has added up to the importance of optical methods compared to other contemporary methods [25–31].

Fe^{3+} , being one of the important trace elements, helps in carrying oxygen through the heme group, but its deficiency and overdose can lead to anemia and hemochromatosis, respectively [32]. Since iron is a bioactive species [33], it becomes necessary to distinguish one oxidation state from the other to assess their course of action, as there are different properties attributed to the different oxidation states. Many probes for the simultaneous detection of Fe^{2+} and Fe^{3+} are reported in the literature [34–42] whereas a smaller number is known with the capability of discriminating the two oxidation states [43–45]. Apart from the biologically important ions, there are many toxic metal ions, which can cause severe damage even at very low concentration. In this context, Hg^{2+} is considered as one of the most important toxic metal ions, as it can lead to damage of kidney, liver, and neurological systems leading to pyrexia [46,47]. Therefore, building up a potential practical sensor system, which efficiently determines toxic metal ions, is the focal point of supramolecular chemistry.

Niu and his co-workers recently developed several fluorescent chemosensors for the detection of various metal cations including Hg^{2+} and Fe^{3+} ions [48–55]. Some fluorescent chemosensors have also been reported for the simultaneous detection of Hg^{2+} and Fe^{3+} species in the literature [56–60]. However, to the best of our knowledge, our probe is the 1st example of a ferrocene-appended fluorescein moiety connected through a triazole linker, which is found to detect Hg^{2+} and Fe^{3+} ions simultaneously. Our continuous research interest in the field of triazole-appended ferrocene-based electrochemical and fluorescence chemosensors led us to rationally design a functionalized fluorescein derivative attached to a ferrocene backbone to develop an easy and reliable chemosensor, with good sensitivity, selectivity and ease of applicability in real samples.

2. Experimental section

2.1. Materials and reagents

The perchlorate salts of Li^+ , Na^+ , K^+ , Fe^{2+} , Fe^{3+} , Cu^{2+} , Hg^{2+} , as well as 1,8-diazabicyclo[5.4.0]undec-7-ene (DBU) and CuI were purchased from Sigma Aldrich and used directly without further purification. The perchlorate salts of Ag^+ , Ca^{2+} , Mg^{2+} , Mn^{2+} , Zn^{2+} , Pb^{2+} , Co^{2+} , Cr^{3+} , Al^{3+} , and *n*-butyllithium (1.6 M in hexane) were purchased from Alfa Aesar. Ferrocene, *N,N,N',N'*-tetramethylethylenediamine (TMEDA), propargyl bromide, fluorescein, NaN_3 , NaBH_4 , K_2CO_3 were purchased from local chemical providers. DMF and acetonitrile (HPLC) were purchased from Thermo Fisher Scientific and freshly distilled prior to use. Chromatography was carried out using 60–120 mesh silica gel in a column of 2.5 cm diameter. All the necessary solvents were dried by conventional methods and distilled under N_2 atmosphere before use. 1,1'-Bis(azidomethyl)ferrocene was synthesized as per the literature procedure [61,62]. The cyclic voltammetry (CV) was performed with a conventional three electrode configuration consisting of glassy carbon as working electrode, platinum as an auxiliary electrode and Ag/Ag^+ as a reference electrode. The experiment was carried out with 10^{-5} M solution of sample in $\text{CH}_3\text{CN}/\text{H}_2\text{O}$ (3/7) containing 0.1 M (TBAP) [$(n\text{-C}_4\text{H}_9)_4\text{NClO}_4$] as supporting electrolyte. The working electrode was cleaned after each run. The cyclic voltammograms were recorded at a scan rate of 0.05 Vs^{-1} . The UV–vis spectra were recorded in $\text{CH}_3\text{CN}/\text{H}_2\text{O}$ (3/7, *v/v*) solutions at $c = 10^{-5}$ M and the fluorescence spectra were recorded at $c = 10^{-7}$ M, as it is stated in the corresponding Figure captions.

2.2. Instrumentation

^1H and ^{13}C NMR spectra were obtained with BRUKER 400 MHz FT-NMR spectrometer, and the chemical shifts are reported in ppm, using tetramethylsilane or the following residual solvent peaks as an internal reference: $\text{CDCl}_3 = 7.26$ (^1H), 76.16 (^{13}C). For ^1H NMR, coupling constants *J* are given in Hz and the resonance multiplicity is described as s (singlet), d (doublet), t (triplet), m (multiplet). The absorption spectra were recorded with a SHIMADZU-2450 UV–vis spectrophotometer at room temperature. Fluorescence was recorded with a HORIBA Scientific Fluoromax-4 Spectrophotometer. CH Instruments Electrochemical Analyzer was used to perform the cyclic voltammetry (CV) and differential pulse voltammetry (DPV) studies. HRMS were taken using a Quadrupole-TOF (Q-TOF) micro MS system using the electrospray ionization (ESI) technique. CHN analysis was performed on a Vario EL elemental CHNS analyser. Melting points were measured in a Labotech melting point apparatus as well as manually by thermometer in silicon oil.

Caution! Metal perchlorate salts are potentially explosive in certain conditions. All due precautions should be taken while handling perchlorate salts!

2.3. Synthesis of compound 4

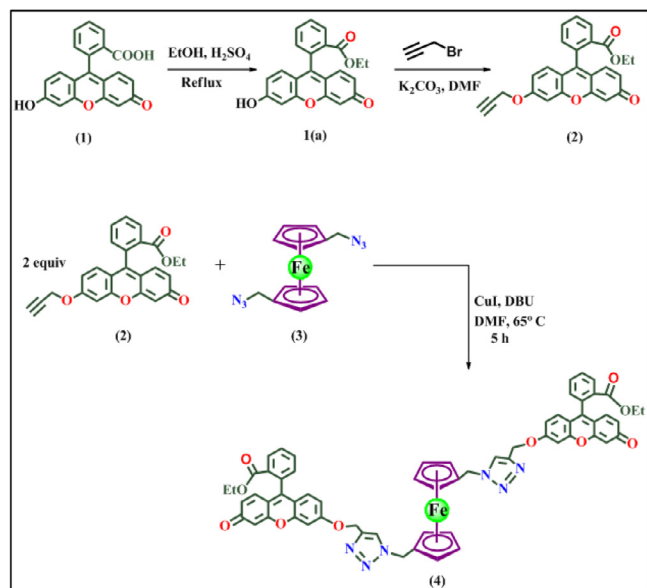
A solution of ethyl 2-(3-oxo-6-(prop-2-yn-1-yloxy)-3*H*-xanthen-9-yl)benzoate, **2** (0.268 g, 0.674 mmol) and 0.5 equiv of 1,1'-bis(azidomethyl)ferrocene, **3** (0.100 g, 0.337 mmol) were taken in a Schlenk flask equipped with a stirrer bar. It was degassed for 30 min. After that CuI (0.4 equiv) and DBU (0.5 equiv) were added to it and the resulting solution was heated at 65°C for 5 h, where upon it was diluted with methanol/water (1:1, *v/v*) and extracted with dichloromethane. The combined organic extracts were washed with brine (50 mL) dried with Na_2SO_4 and the solvent was removed in vacuo to afford a yellow residue. Purification by column chromatography on silica gel with EtOAc/hexane (8:2, *v/v*) as the eluent afforded a yellow solid compound **4** (0.316 g, 85.86%).

4: ^1H NMR (CDCl_3 , 400 MHz): $\delta = 8.25\text{--}8.22$ (m, 2H, $H_{\text{fluorescein}}$), 7.73–7.69 (m, 2H, $H_{\text{fluorescein}}$), 7.68–7.64 (m, 2H, $H_{\text{fluorescein}}$), 7.61 (s, 2H, H_{triazole}), 7.28 (d, 2H, $H_{\text{fluorescein}}$, $J = 7.6$ Hz), 7.06 (d, 2H, $H_{\text{fluorescein}}$, $J = 1.2$ Hz), 6.90–6.82 (m, 4H, $H_{\text{fluorescein}}$), 6.79–6.76 (m, 2H, $H_{\text{fluorescein}}$), 6.54–6.52 (m, 2H, $H_{\text{fluorescein}}$), 6.43 (d, 2H, $H_{\text{fluorescein}}$, $J = 1.6$ Hz), 5.25 (d, 8H, CH_2 , $J = 1.6$ Hz), 4.26 (s, 4H, H_{Cp}), 4.01 (q, 4H, OCH_2ester , $J = 7.2$ Hz), 0.95 (t, 6H, OCH_2CH_3 , $J = 7.2$ Hz); ^{13}C NMR (CDCl_3 , 100 MHz): $\delta = 185.7$, 165.3, 162.4, 158.9, 154.0, 150.3, 142.6, 134.1, 132.7, 132.6, 131.2, 131.1, 130.6, 130.5, 130.4, 129.9, 129.7, 129.1, 129.0, 122.8, 117.8, 115.3, 113.6, 105.7, 101.4, 101.3, 82.0, 70.0, 69.6, 62.3, 61.4, 52.4, 49.7, 13.6. Mp: $195\text{--}197^\circ\text{C}$. HRMS (ESI) *m/z* calcd for $\text{C}_{62}\text{H}_{48}\text{FeN}_6\text{O}_{10}$ [$\text{M} + 23$] $^+$ 1115.2681; found 1115.2626; Anal. Calcd for $\text{C}_{62}\text{H}_{48}\text{FeN}_6\text{O}_{10}$ C, 68.12; H, 4.43; N, 7.69. Found: C, 68.02; H, 4.28; N, 7.34.

3. Results and discussion

3.1. Synthesis of receptor 4

Our long-term interest in the synthesis and study of the reactivity of the triazole moiety has led us to the exploration of a novel and simple triazole-appended ferrocene derivative (**4**) starting from the corresponding alkyne and azide. Receptor **4**, having a ferrocene skeleton, has been synthesized by following the synthetic route as depicted in Scheme 1. A click reaction between 2 equiv. of ethyl 2-(3-oxo-6-(prop-2-yn-1-yloxy)-3*H*-xanthen-9-yl)benzoate (**2**) and 1,1'-bis(azidomethyl)ferrocene (**3**) yielded receptor **4**, which was well-characterized using various spectroscopic techniques such as ^1H NMR, ^{13}C NMR, HRMS and elemental analysis. The HRMS (ESI, Fig. S4) spectrum shows the major peak at *m/z* 1115.2626 [$\text{M} + \text{Na}$] $^+$, which perfectly matches the



Scheme 1. Synthesis of compound 4.

calculated molecular weight of $[L + Na]^+$ (1115.2681). After having obtained compound 4 in good yield, its cation sensing ability has been thoroughly studied by UV-vis, fluorescence spectroscopy, electrochemical studies and colorimetric detection method along with 1H NMR titration.

3.2. UV-vis absorption study

The changes in the UV-vis absorption spectra of receptor 4 in solution of CH_3CN/H_2O (10^{-5} M, 3/7) in the presence of perchlorate salts of K^+ , Na^+ , Ag^+ , Fe^{2+} , Fe^{3+} , Al^{3+} , Cr^{3+} , Co^{2+} , Cu^{2+} , Zn^{2+} , Ca^{2+} , Mg^{2+} , Mn^{2+} , Cd^{2+} , Ni^{2+} , Hg^{2+} and Pb^{2+} ions were measured and recorded (ESI, Fig. S5). As shown in Fig. 1, a very weak band above 350 nm is ascribed to a trace amount of the ring-open form of 4 [63] and the bands at 430, 454 and 485 nm are the characteristic peaks of the fluorescein moiety itself [64]. The peak at 454 nm is attributed to the $\pi-\pi^*$ transition of the fluorescein chromophore [65]. Addition of 1 equiv. each of Hg^{2+} and Fe^{3+} to the receptor 4 separately has noticeably reduced the intensity of the band at 485 nm with a concomitant appearance of a new peak at 430 nm. Two well-defined isosbestic points were observed at 404 and 451 nm for Hg^{2+} and at 422 and 447 nm for Fe^{3+} , indicating a net inter-conversion between un-complexed and

complexed species. Moreover, the absorbance at 430 nm remained constant in the presence of more than 1 equiv. of Fe^{3+} or Hg^{2+} , strongly suggesting the formation of 1:1 ligand-to-metal complexes. Furthermore, the formation of a 1:1 complex of 4 with Hg^{2+} and Fe^{3+} ion was confirmed by elemental analysis of the isolated $[4Hg^{2+}]$ and $[4Fe^{3+}]$ species. A linear regression plot has been obtained from the absorption intensity of the ligand versus metal ion concentrations and indeed, a linear increment of absorption intensity up to 1 equiv. for both metal ions was observed (ESI, Fig. S6).

3.3. Fluorescence study

To further carry forward our investigation of interaction of receptor 4 with Hg^{2+} and Fe^{3+} ions, the fluorescence emission spectra were measured in CH_3CN/H_2O (3/7, v/v) at 25 °C, (Fig. 2). The unaltered fluorescence spectra of 4 upon addition of any of the aforementioned cations, except Hg^{2+} and Fe^{3+} ions, infer us the selectivity of our probe (ESI, Fig. S7). On excitation at 430 nm, in the absence of any analyte, the probe displayed emission peaks at 521 and 545 nm which are typical for the fluorescein moiety [66,67]. Addition of Hg^{2+} and Fe^{3+} generates a new emission peak at 473 nm corresponding to the binding of metal ions to the receptor 4. With the increasing concentration of Hg^{2+} ion up to 1 equiv., the fluorescence intensity at 473 nm gradually increases, while that at 521 and 545 nm decreases. However, the change in fluorescence intensity at 545 nm outweighs change in fluorescence intensity at 521 nm. Therefore, a change in ratio of the fluorescence intensities at the two wavelengths (545 nm and 473 nm) is considered to explain the ratiometric phenomenon. As the ratio change at 545 nm and 473 nm is the key factor in the detection of Hg^{2+} and Fe^{3+} ions, the probe 4 is considered a ratiometric probe. The fluorescence intensity ratio of 4 (I_{473}/I_{545}) and its metal derivatives shows a linear relationship (R^2 greater than 0.99) with increasing concentrations of Hg^{2+} and Fe^{3+} ions (Fig. 3). Addition of an excess amount of analyte beyond 1 equiv. did not exhibit any further changes in the fluorescence intensities. This 1:1 ligand-to-metal binding ratio was further verified via Job's plot for both $[4Hg^{2+}]$ and $[4Fe^{3+}]$ species (ESI, Figs. S8 and S9). The association constant (K_a) was calculated to be $3.35 \times 10^5 M^{-1}$ and $2.67 \times 10^5 M^{-1}$ for Hg^{2+} and Fe^{3+} respectively according to a fit plot [68] (ESI, Figs. S10 and S11).

The sensitivity of a probe is determined by its quantitative response to a particular species. To investigate the sensitivity of probe 4, fluorescence titration experiments were carried out with Fe^{3+} and Hg^{2+} ions (4.87×10^{-7} M). A good linear relationship between the fluorescence intensity ratio (data extracted from Fig. 2) and the concentration of Fe^{3+} and Hg^{2+} was presented with $R^2 = 0.992$ and 0.972 for Fe^{3+} and Hg^{2+} respectively (ESI, Fig. S12). The limits of detection (LOD)

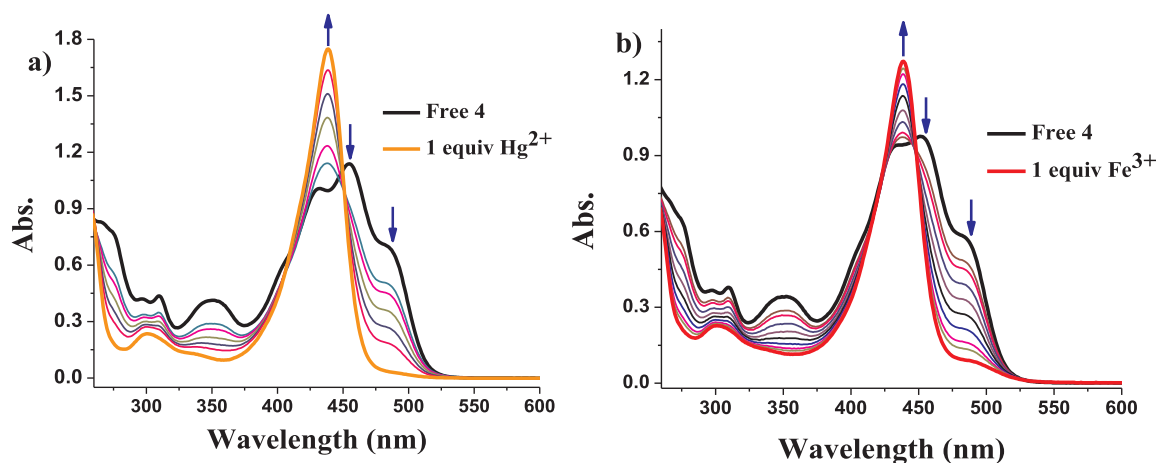


Fig. 1. Changes in the absorption spectra of 4 in CH_3CN/H_2O (3/7, v/v) (10^{-5} M) at room temperature and pH = 7.2, upon addition of increasing amounts of (a) Hg^{2+} and (b) Fe^{3+} ions up to 1 equiv.

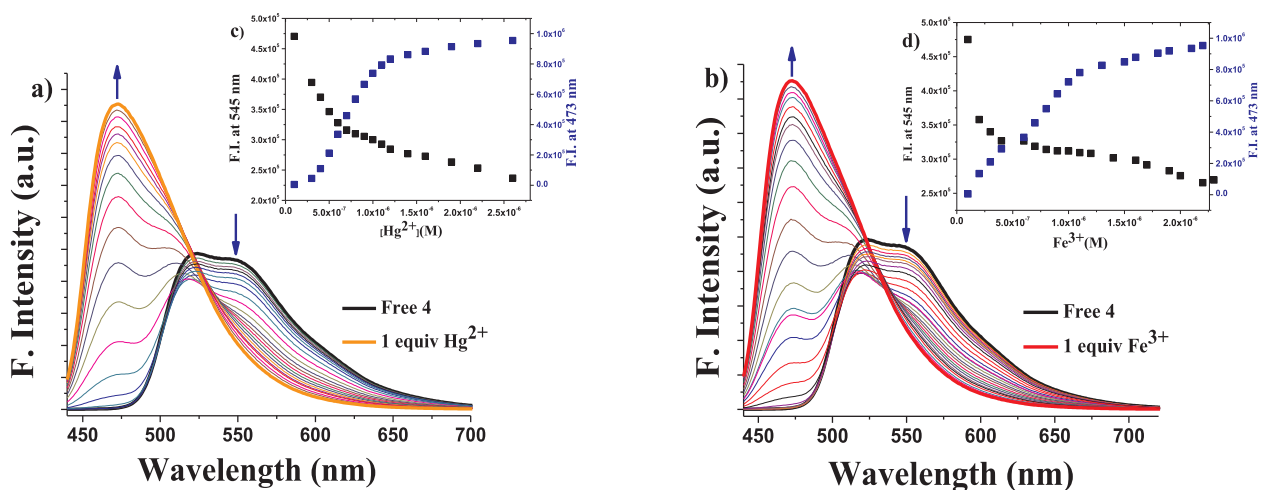


Fig. 2. (a) Fluorescence emission titration of compound **4** (10^{-7} M) upon addition of Hg^{2+} ion and (b) Fe^{3+} ion up to 1 equiv. in $\text{CH}_3\text{CN}/\text{H}_2\text{O}$ (3/7; v/v) solution at room temperature and pH = 7.2. Inset of Fig. 2; shows the plot of emission intensity variation at 473 and 545 nm (c) as a function of Hg^{2+} concentration, (d) as a function of Fe^{3+} concentration respectively.

were calculated by the widely used $3\sigma/S$ method [69] where ‘ σ ’ is the standard deviation of the blank and ‘ S ’ is the slope of the calibration curve. The LOD was found to be 9.75×10^{-8} M and 39×10^{-8} M for Fe^{3+} and Hg^{2+} ions respectively.

Further, in order to compare our probe with the other reported probes, we have thoroughly searched the literature and tabulated the data in Table 1, demonstrating that our probe is comparable or even better than other reported fluorescein-based Hg^{2+} and Fe^{3+} ion sensor molecules. Further, from the literature survey, it is evident that the present probe **4** is highly selective as it recognizes only two metal ions among various other metal ions and is fairly sensitive on the basis of its corresponding low limits of detection and high binding constant values. Moreover, this is the 1st example of a ferrocene based-fluorescein derivative for the simultaneous detection of Hg^{2+} and Fe^{3+} ions in the literature.

3.4. Temperature, time and pH effect

To investigate the range of applicability of the ligand in metal sensing, temperature, time and pH effects on the bare ligand as well as of the metal-bonded probe have been studied [80–82] in CH_3CN medium. The temperature of CH_3CN solutions of ligand **4**, $[\text{4Hg}^{2+}]$ and $[\text{4Fe}^{3+}]$ has been increased gradually from room temperature to 80°C . In case of free ligand, the fluorescence intensity was almost unaffected with rising temperature (ESI, Fig. S13). This suggests that the probe is

very stable in the temperature range of 25°C to 80°C . For $[\text{4Hg}^{2+}]$ and $[\text{4Fe}^{3+}]$, the fluorescence intensity remains the same up to 60°C and decreases abruptly beyond 60°C (ESI, Fig. S13). These results demonstrate that Hg^{2+} and Fe^{3+} complexes of probe **4** are stable over a wide temperature range of 25°C to 60°C .

To determine the sensitivity of a colorimetric or fluorescence probe, response time plays a significant role. Thus, the effect of time on the fluorescence intensity of probe **4** (10^{-7} M) has been determined in CH_3CN solvent (Fig. 4). Upon addition of 1 equiv. of $\text{Hg}^{2+}/\text{Fe}^{3+}$ ion (10^{-7} M), the ratio of fluorescence intensities increases instantaneously and reaches a maximum value within 40 s for Hg^{2+} and 30 s for Fe^{3+} ion. Fluorescence intensities remain constant over an extended period of time (200 s). This suggests that the present probe **4** may provide a proficient “zero-wait” detection method for the detection of Hg^{2+} and Fe^{3+} ions.

Fluorescence intensities of ligand **4**, $[\text{4Hg}^{2+}]$ and $[\text{4Fe}^{3+}]$ were measured in the pH range of 2–12 (ESI, Fig. S14). The fluorescence intensities remain constant over the neutral pH range i.e. within pH 6–7. However, changes in fluorescence intensity were observed in the acidic or basic pH range as the fluorescein moiety is sensitive to pH changes [83] due to the presence of sensitive functional groups. Therefore, the sensing ability of a fluorescein-based sensor is expected to be found precisely in the neutral pH range only. From the plot of fluorescence intensity vs pH of metal-bound ligand, it is evident that the present probe **4** can bind to Hg^{2+} and Fe^{3+} most effectively at neutral

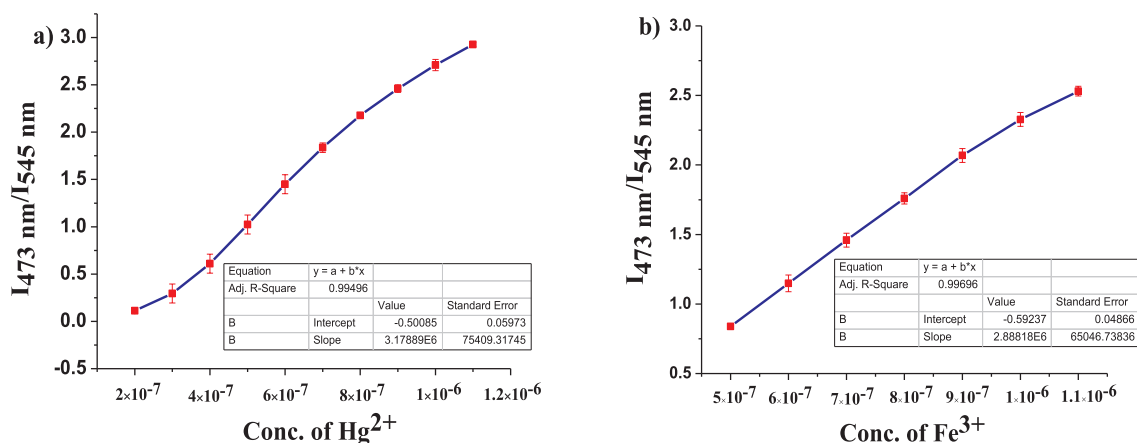


Fig. 3. Linear graph representation of fluorescence intensity ratio of receptor **4** for (a) Hg^{2+} and (b) Fe^{3+} ions.

Table 1
Comparison of the analytical parameters of compound 4 with other reported fluorescein-based Hg²⁺ and Fe³⁺ sensors.

Sl no.	Ligand Molecular Formula	Analyte	Method of Detection	Color change	Detection Limit	Binding Constant	Sensitivity	Reference
1	C ₂₂ H ₂₂ N ₃ O ₈ S	Fe ³⁺ & Hg ²⁺	Turn-Off fluorescence	Green to colorless for Fe ³⁺	7.92 × 10 ⁻⁸ M for Fe ³⁺ 4.22 × 10 ⁻⁸ M for Hg ²⁺	3.37 × 10 ⁸ M ⁻² for Fe ³⁺ 8.41 × 10 ⁴ M ⁻² for Hg ²⁺	High	[70]
2	C ₁₉ H ₁₂ NOS ₃	Fe ²⁺ & Hg ²⁺	Turn-On fluorescence	Green to strong green	13.4 nM for Fe ³⁺ 61.7 nM for Hg ²⁺	1.34 × 10 ⁶ M ⁻¹ for Fe ³⁺ 8.99 × 10 ⁶ M ⁻¹ for Hg ²⁺	High	[56]
3	C ₂₈ H ₂₈ N ₂ O ₂ S	Fe ³⁺ & Hg ²⁺	Colorimetric	Orange to cream yellow Orange to grain yellow	0.538 μM for Fe ³⁺ 1.689 μM for Hg ²⁺	1.24 × 10 ⁶ M ⁻¹ for Fe ³⁺ 1.1 × 10 ⁶ M ⁻¹ for Hg ²⁺	Medium	[71]
4	C ₄₇ H ₄₁ N ₅ O ₄	Fe ³⁺ & Hg ²⁺	Turn-On fluorescence	Colorless to transparent pink	2.72 × 10 ⁻⁸ M for Fe ³⁺ 9.08 × 10 ⁻⁸ M for Hg ²⁺	4.95 × 10 ⁻⁷ M ^{3/2} for Fe ³⁺ and 6.68 × 10 ⁻⁸ M ^{3/2} for Hg ²⁺	High	[72]
5	C ₁₈ H ₂₃ N ₃ O ₄ S	Hg ²⁺ & Fe ³⁺	Ratiometric fluorescence	Yellow to purple Yellow to red	5 × 10 ⁻³ M for Hg ²⁺	-	Low	[73]
6	C ₃₃ H ₃₃ N ₅ O ₄ S	Fe ³⁺ & Hg ²⁺	Turn-Off fluorescence	-	130 nM for Fe ³⁺ 302 nM for Hg ²⁺	3.8 × 10 ⁴ M ⁻¹ for Fe ³⁺ 5.3 × 10 ⁴ M ⁻¹ for Hg ²⁺	High	[74]
7	C ₃₆ H ₅₂ N ₇ O ₅	Fe ³⁺ & Hg ²⁺	Turn-Off- Hg ²⁺ Ratiometric-Fe ³⁺	Colorless to pink	4.6 × 10 ⁻⁶ M for Fe ³⁺ 4.8 × 10 ⁻⁶ M for Hg ²⁺	2.66 × 10 ³ M ⁻¹ for Fe ³⁺ 9.29 × 10 ⁴ M ⁻¹ for Hg ²⁺	Medium	[75]
8	C ₃₄ H ₅₂ N ₇ O ₄	Fe ³⁺ & Hg ²⁺	Turn-On fluorescence	Colorless to pink	5.7 × 10 ⁻⁷ M for Fe ³⁺ 2.72 × 10 ⁻⁶ M for Hg ²⁺	3.4 × 10 ⁵ M ⁻¹ for Hg ²⁺	Medium	[76]
9	C ₂₉ H ₃₃ N ₂ O	Fe ³⁺ & Hg ²⁺	Turn-Off fluorescence	Colorless to yellow	54.76 × 10 ⁻⁵ M for Fe ³⁺ 7.01 × 10 ⁻⁶ M for Hg ²⁺	1.64 × 10 ⁴ M ⁻¹ for Fe ³⁺ 3.79 × 10 ⁴ M ⁻¹ for Hg ²⁺	Low	[77]
10	C ₂₆ H ₁₈ N ₂ O ₂ S ₃	Fe ³⁺ & Hg ²⁺	Turn-On fluorescence	Khaki to reddish brown for Hg ²⁺	3.52 × 10 ⁻⁸ M for Fe ³⁺ 5.0 × 10 ⁻⁸ M for Hg ²⁺	3.10 × 10 ⁵ M ⁻² for Fe ³⁺ 2.13 × 10 ⁵ M ⁻² for Hg ²⁺	High	[78]
11	C ₁₇ H ₁₂ N ₄ O ₂	Fe ³⁺ , Hg ²⁺ & Cu ²⁺	Turn-On fluorescence	-	8 × 10 ⁻⁷ mol/L ⁻¹ for Fe ³⁺	-	High	[79]
12	C ₃₄ H ₃₂ N ₁₆ O ₆ B ₂ F ₄	Fe ³⁺ & Hg ²⁺	Turn-On fluorescence	Red to yellow	3.91 × 10 ⁻⁷ M for Fe ³⁺ 7.74 × 10 ⁻⁸ M for Hg ²⁺	-	High	[57]
13	C ₃₃ H ₄₆ N ₁₅ O ₄ B ₃ F ₆	Fe ³⁺ & Hg ²⁺	Turn-On fluorescence	-	6.68 × 10 ⁻⁸ M for Fe ³⁺ 2.24 × 10 ⁻⁷ M for Hg ²⁺	-	High	[58]
14	C ₂₀ H ₂₂ N ₂ S ₂	Fe ³⁺ & Hg ²⁺	Turn-Off fluorescence	-	0.3 μM for Fe ³⁺ 0.5 μM for Hg ²⁺	2.80 × 10 ⁴ M ⁻¹ for Fe ³⁺ 3.27 × 10 ¹⁰ M ⁻² for Hg ²⁺	Medium	[59]
15	DHB; α-CD	Fe ²⁺ & Hg ²⁺	Turn-On fluorescence	Colorless to deep brown and faint brown	0.5 × 10 ⁻⁷ M for Fe ³⁺ 1.0 × 10 ⁻⁷ M for Hg ²⁺	1.82 × 10 ⁴ M ⁻¹ for Fe ³⁺ 3.16 × 10 ⁴ M ⁻¹ for Hg ²⁺	High	[60]
16	C ₆₂ H ₄₈ FeN ₆ O ₁₀	Hg ²⁺ & Fe ³⁺	Ratiometric fluorescence & Electrochemical	Yellow to blue in both the case	9.75 × 10 ⁻⁸ M for Fe ³⁺ 39 × 10 ⁻³ M for Hg ²⁺	2.67 × 10 ⁵ M ⁻¹ for Fe ³⁺ 3.35 × 10 ⁵ M ⁻¹ for Hg ²⁺	High	Present work

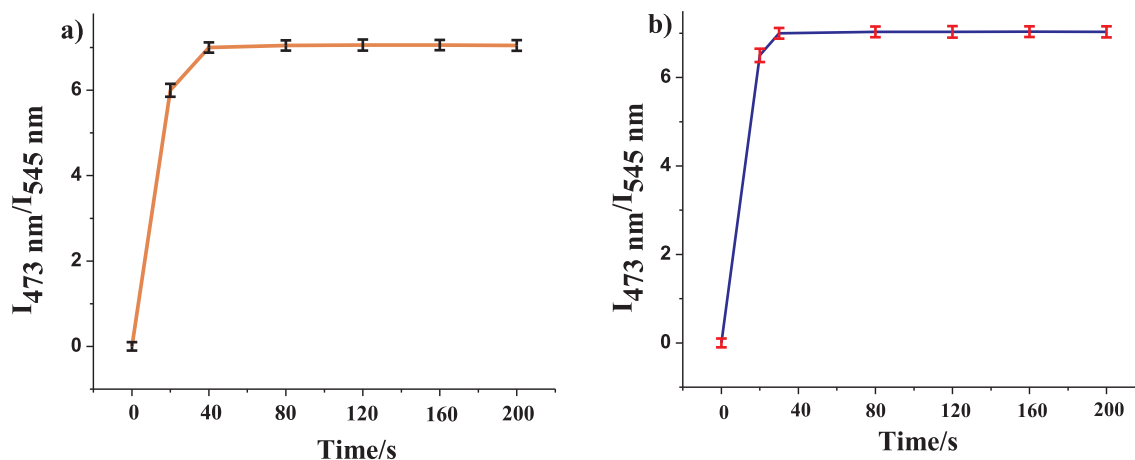


Fig. 4. Reaction time profile: changes of fluorescence intensity of receptor **4** (10^{-7} M) in the presence of 1 equiv. of (a) Hg^{2+} and (b) Fe^{3+} ions as a function of time (0–200 s).

pH.

3.5. Solvatochromism of receptor **4**

Investigation of the solvatochromic effect of **4** in selected organic solvents yielded some interesting results. Although the structured absorption bands at ca. 430, 454, 485 nm and emission bands at 521 and 545 nm of compound **4** correspond to characteristics of the quinoid form of fluorescein [84], they are devoid of remarkable wavelength shift in a range of different organic solvents. However, a negative solvatochromism is observed for protic solvents like ethanol, which can be explained by the larger charge separation and therefore larger dipole moment of the excited state as compared to the ground state. Hence, there occurs a decrease in the energy state difference on going from polar to non-polar solvent [85–87]. It is worth noticing that hydrogen bonding between the fluorescein moiety within our structured framework and the polar solvent led to a hypsochromic shift of the absorbance as well as fluorescence emission band (Fig. 5).

3.6. Electrochemical study

The electrochemical properties of receptor **4** were investigated by cyclic voltammetry (CV) and differential pulse voltammetry (DPV) in $\text{CH}_3\text{CN}/\text{H}_2\text{O}$ (3/7, 10^{-5} M). Remarkably, the presence of a range of other metal ions (as perchlorate salts) as mentioned above was examined for the electrochemical behavior in $\text{CH}_3\text{CN}/\text{H}_2\text{O}$ (3/7, v/v) containing 0.1 M $[(n\text{-Bu})_4\text{N}]\text{ClO}_4$ as supporting electrolyte (ESI, Fig.

S15). The addition of Hg^{2+} and Fe^{3+} gave a clean response with receptor **4**. The free receptor exhibited a reversible one-electron redox wave, typical of a ferrocene derivative, with the half-wave potential value $E_{1/2} = 0.615$ V for **4** due to the ferrocene/ferrocenium redox couple. After addition of 1 equiv. of Hg^{2+} or Fe^{3+} , respective anodic shifts of $\Delta E_{1/2} = 33$ mV and 31 mV were observed due to the formation of new complex species (Figs. 6a and 7a). Also, a differential pulse voltammetry (DPV) titration study was performed for a better understanding of the interaction of the Hg^{2+} and Fe^{3+} ions with receptor **4**, and the results are concurrent with that obtained from the cyclic voltammetry study (Figs. 6b and 7b).

Cyclic voltammetry is one of the analytical tools that allows calculating the detection limit of a probe. Thus, to analyze the LOD we have plotted the linear calibration graph between the change in potential difference ($\Delta E_{1/2}$) vs conc. of increasing amount of metal ions in $\text{CH}_3\text{CN}/\text{H}_2\text{O}$ (3/7) as a solvent (ESI, Fig. S16). A linear response was observed in the concentration range of 10^{-5} M from the calibration plot. LODs were calculated by using the equation [88] ($(3\sigma/S)$; σ = standard deviation and S = slope of the calibration plot) and were found to be 13.7×10^{-8} M and 30×10^{-8} M and for Fe^{3+} and Hg^{2+} ions, respectively. These values are almost consistent with those of obtained from the fluorescence plot.

3.7. Naked eye detection

Visual detection by naked eye, one of the preliminary techniques for the metal cation binding study, was performed via colorimetric

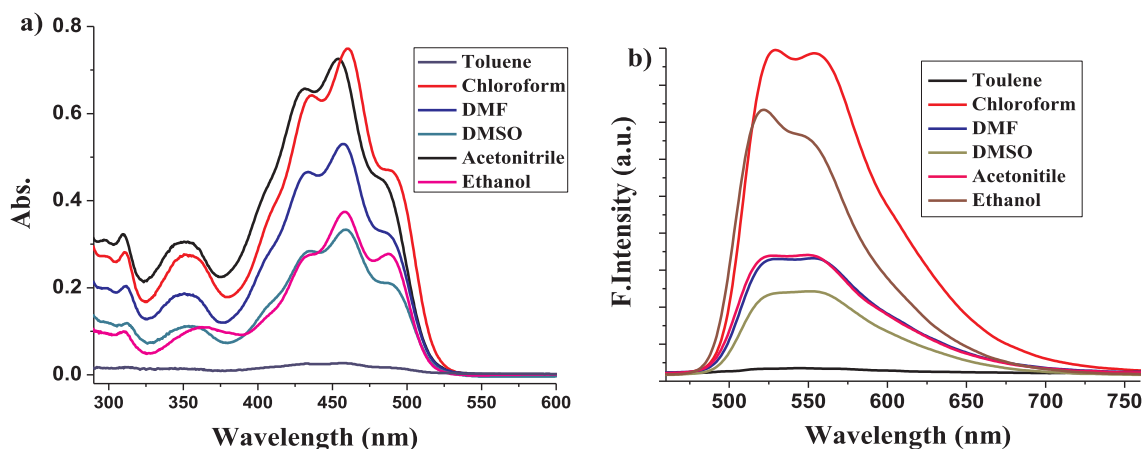


Fig. 5. (a) UV-vis absorption and (b) fluorescence spectra of **4** in various solvents at room temperature and pH = 7.2.

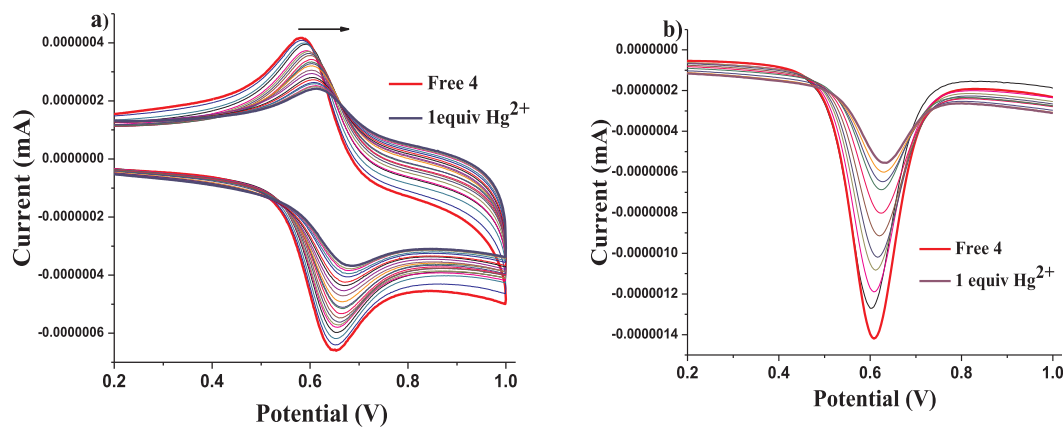


Fig. 6. (a) Evolution of CV and (b) DPV of **4** (10^{-5} M) in $\text{CH}_3\text{CN}/\text{H}_2\text{O}$ (3/7) at room temperature and $\text{pH} = 7.2$, using $[(n\text{-Bu})_4\text{N}]\text{ClO}_4$ as supporting electrolyte on addition of 1 equiv. of Hg^{2+} scanned at 0.05 V s^{-1} .

experiments with $\text{CH}_3\text{CN}/\text{H}_2\text{O}$ (3/7) solutions of **4** (10^{-5} M) with the different metal cations. Distinctive color changes from yellow to faint green for both Hg^{2+} and Fe^{3+} ions with probe **4** were observed during the investigation with 1 equiv. of perchlorate salts of different metal cations (Na^+ , Ag^+ , Ca^{2+} , Mg^{2+} , Mn^{2+} , Hg^{2+} , Fe^{2+} , Fe^{3+} , Al^{3+} , Cr^{3+} , Co^{2+} , Cu^{2+} , Zn^{2+} , Cd^{2+} , Ni^{2+} and Pb^{2+}) (Fig. 8), which indicates the selective and sensitive 'naked eye' identifying capacity of receptor **4** for Hg^{2+} and Fe^{3+} ions.

3.8. Studies on the reversibility of the Hg^{2+} and Fe^{3+} binding to receptor **4**

For a superior sensor molecule the important perspectives are to recognize a particular analyte (selectivity), a low limit of detection (sensitivity), and reversibility. For the reversibility point of view, a fluorescence study for the Hg^{2+} and Fe^{3+} ions has been performed by exposing the Hg^{2+} ion to the solution of **4**. A greenish blue color emanates with enhancing fluorescence intensity, which reverses back to its nearly original form upon the introduction of iodide as a sequestering agent to the solution, owing to the formation of HgI_2 . Repeated changes in color and fluorescence intensity on further addition of Hg^{2+} and masking it by the sequestering agent proves the reversible nature of the interaction of receptor **4** with the Hg^{2+} ion (ESI, Fig. S17). Similarly, the reversibility of the sensing of the Fe^{3+} ion was explored using EDTA as the binding agent (ESI, Fig. S18). In both the cases, the above experiments can be repeated at least 3 times without much loss in sensitivity.

Ease of applicability of a sensor is a quality that makes it more

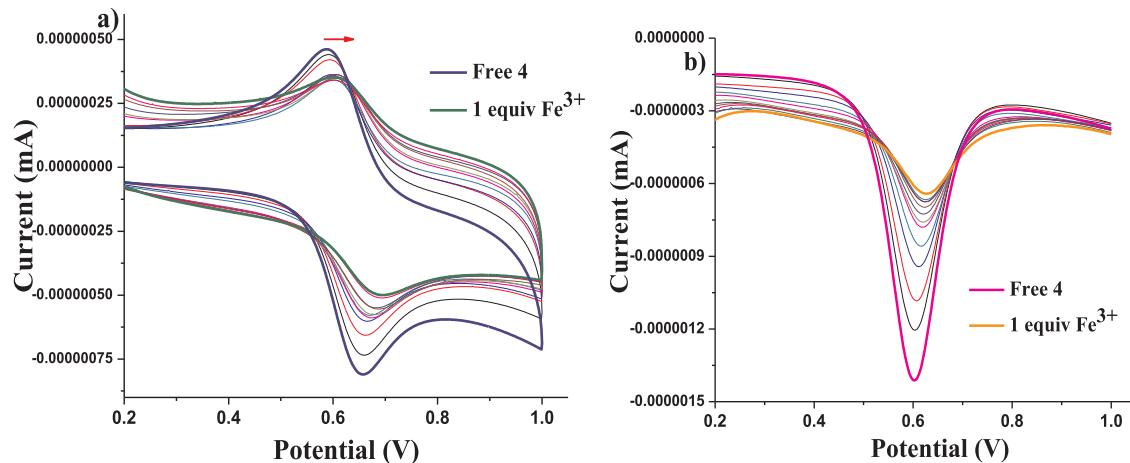


Fig. 7. (a) Evolution of CV of **4** (10^{-5} M) and (b) DPV of **4** (10^{-5} M) in $\text{CH}_3\text{CN}/\text{H}_2\text{O}$ (3/7) at room temperature and $\text{pH} = 7.2$, using $[(n\text{-Bu})_4\text{N}]\text{ClO}_4$ as supporting electrolyte on addition of 1 equiv. of Fe^{3+} scanned at 0.05 V s^{-1} .

convenient to use. Keeping this idea in mind, we have set out to investigate the action of receptor **4** on a solid support of silica, which demonstrates its practical analytical applicability. Here, the silica gel (60–120 mesh, 6.0 g, colorless), soaked with **4** (10^{-3} M) in 15 mL of acetonitrile and dried, was added to aqueous solutions of Hg^{2+} and Fe^{3+} ions (10^{-3} M) separately. The faint yellow color of the treated silica gel instantly changed to green upon treatment with Hg^{2+} and Fe^{3+} ions (Fig. 9). This experiment clearly demonstrates the practical applicability of the present probe for the development of material-based sensors.

A competitive experiment of compound **4** with other metal ions was carried out using the fluorescence emission study, inferring that receptor **4** displays a high specificity towards only Hg^{2+} and Fe^{3+} ions. Further, another competition experiment was performed between Hg^{2+} and Fe^{3+} ions with probe **4** to ascertain the particular selectivity towards only one ion. The fluorescence enhancement of the $[\text{4}\cdot\text{Hg}^{2+}]$ system (10^{-7} M) was found to be perturbed in the presence of 1 equiv. of Fe^{3+} ions. However, the fluorescence emission of the $[\text{4}\cdot\text{Fe}^{3+}]$ system did not display any significant change in presence of Hg^{2+} ions (Fig. 10). Therefore, probe **4** could be used for the detection of Fe^{3+} in the presence of other competing metal ions, including the Hg^{2+} ion. In addition, **4** can be utilized for the detection of Hg^{2+} ions in the presence of other competing ions, except for the Fe^{3+} ion.

3.9. Real sample preparation and analysis

The effectiveness of receptor **4** can only be justified when it can

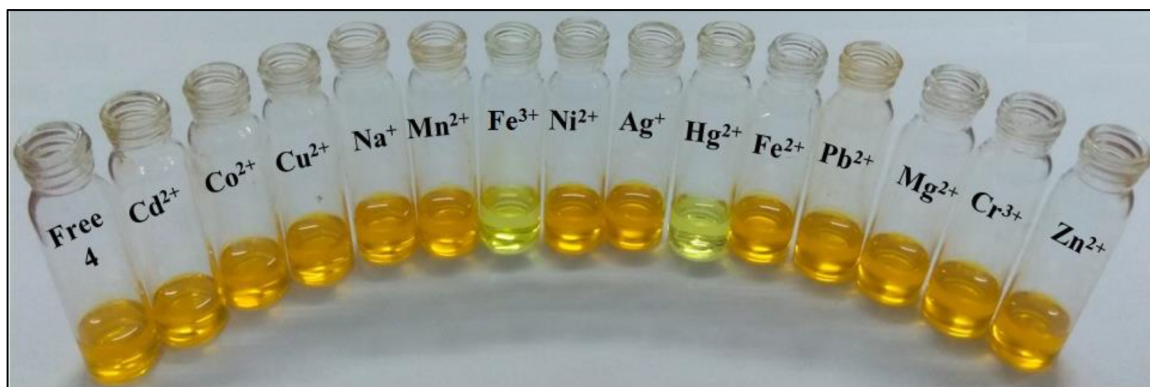


Fig. 8. Visual colour changes observed for 4 in $\text{CH}_3\text{CN}/\text{H}_2\text{O}$ (10^{-5} M) after addition of 1 equiv. of several metal cations.

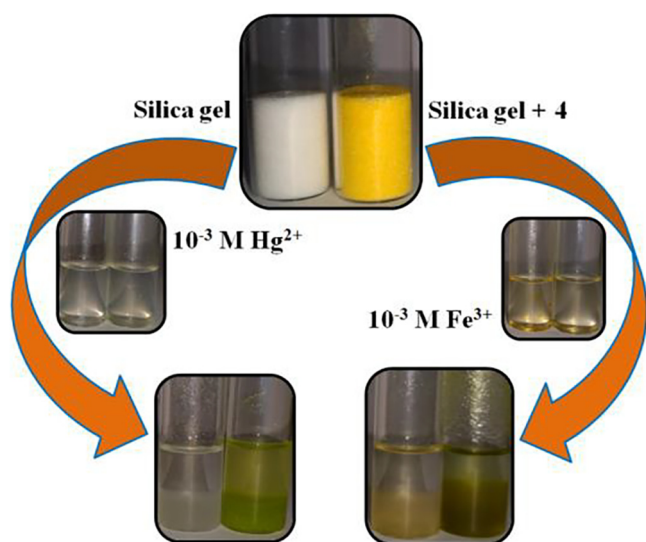


Fig. 9. Color changes of silica gel soaked with 4 upon addition to aqueous solutions of Hg^{2+} ion and Fe^{3+} ion.

sense the selected metal ions in real water samples. For such an experiment, pond water and tap water were collected from Jadavpur University campus area and filtered on a Whatman 41 filter paper to

Table 2

Determination of recovered conc. of Fe^{3+} and Hg^{2+} in pond water and tap water samples.

Samples	Added metal conc. (M)	Recovered metal conc. (M)	% of Recovery	% Error	
Pond water	Fe^{3+}	0.4014×10^{-7}	0.3973×10^{-7}	98.98	1.02
	Hg^{2+}	0.4014×10^{-7}	0.4075×10^{-7}	101.53	1.51
Tap water	Fe^{3+}	0.1991×10^{-7}	0.2031×10^{-7}	102.00	2.00
	Hg^{2+}	0.1739×10^{-7}	0.1787×10^{-7}	102.76	2.76

filter off the unwanted dust particles. The pH of the water samples was maintained around 6.5–7. Known concentrations of Fe^{3+} and Hg^{2+} ions were added to the water samples separately and they were introduced to the receptor 4 to determine recovered concentrations of Fe^{3+} and Hg^{2+} ions, respectively. Fluorescence spectra were recorded after each addition of metal ions to the ligand solution (10^{-7} M) and enhancement of fluorescence intensities was observed for both real samples. With each addition, the corresponding recovered metal ion concentration was calculated from the equations $y = (145.4x + 110.7)$ and $y = (123.5x + 160.7)$, with correlation coefficient $R^2 = 0.962$ and $R^2 = 0.968$ for Fe^{3+} and Hg^{2+} ions respectively for pond water. Equations $y = (254.9x + 126.5)$ and $y = (277.3x + 137.7)$ and correlation coefficient $R^2 = 0.981$ and $R^2 = 0.959$ were found for Fe^{3+} and Hg^{2+} ions respectively for tap water sample (ESI, Figs. S19 and S20). The experimental concentration and percentage recovery values

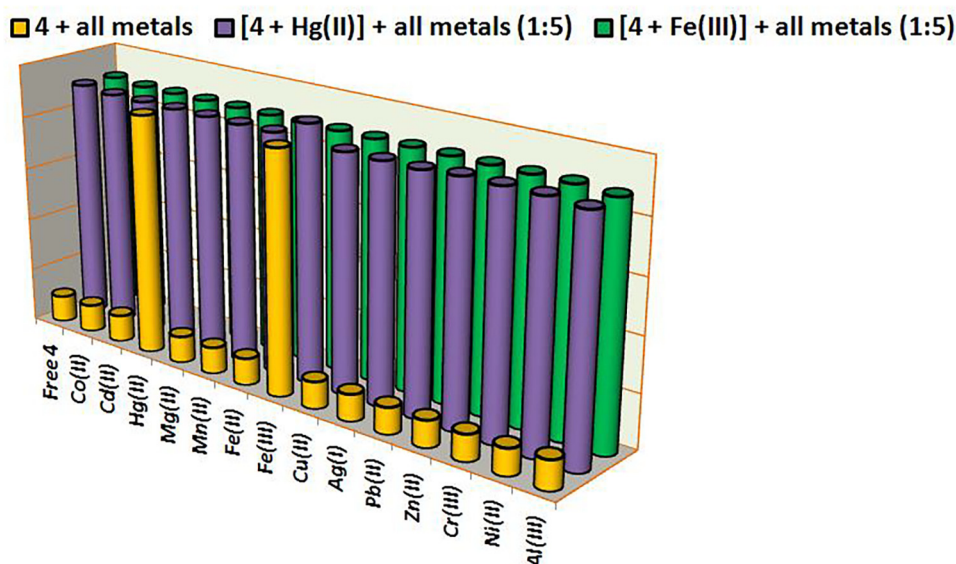


Fig. 10. Bar plot representation of the fluorescence emission intensity of 4 upon the addition of several potentially competing cations (1:5) in $\text{CH}_3\text{CN}/\text{H}_2\text{O}$.

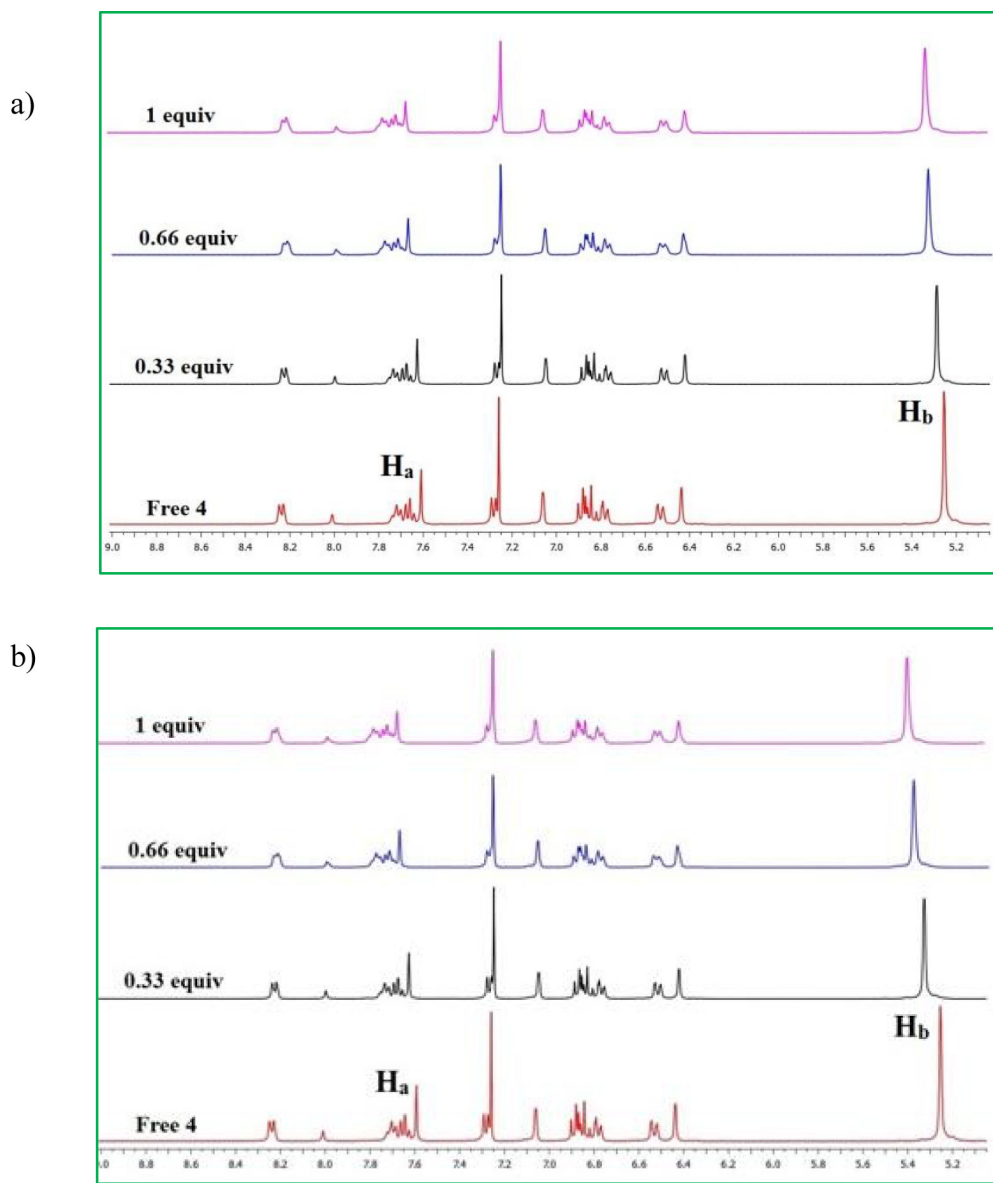


Fig. 11. Proposed binding mode between receptor 4 with (a) Hg^{2+} and (b) Fe^{3+} ions in CDCl_3 .

of the Fe^{3+} and Hg^{2+} ions are shown in Table 2.

3.10. IR and ^1H NMR spectroscopic titration

Further, we have performed FT-IR spectral measurement of free ligand and its complexes with Hg^{2+} and Fe^{3+} ions. Upon addition of metal ions, no significant change or shift in stretching frequency of the carbonyl group as well as any other peak in the finger print region was observed. One new peak appeared at 1103 cm^{-1} which may be attributed to the Cl-O stretching frequency of the ClO_4^- unit (ESI, Fig. S21). This result demonstrated that metals are certainly not binding with to the carbonyl group, they rather bind to other heteroatoms present in the molecule. As an IR spectral titration is not sufficient to demonstrate the binding mode unambiguously for the present probe 4, we have further performed a ^1H NMR titration which is more convincing in order to ascertain a metal ion binding mode.

A preliminary ^1H NMR cation binding analysis of receptor 4 with Hg^{2+} and Fe^{3+} ions was investigated by ^1H NMR spectroscopic titration experiment in CDCl_3 as solvent. Upon addition of 1 equiv. of Hg^{2+} ion to the solution of receptor 4, the H_a proton with an initial chemical shift of 7.60 ppm, corresponding to the triazole unit of the free receptor,

shifted downfield by 0.05 ppm, resulting in a signal at 7.65 ppm. Similarly, the H_b proton attached to the OCH_2 unit experienced a downfield shift of 0.07 ppm, giving rise to a signal at 5.32 ppm (Fig. 11(a)). Interestingly, the other protons of receptor 4, corresponding to the fluorescein moiety, do not show any shift in the ^1H NMR spectrum compared to those of the protons of the unbound receptor. This suggests the possible binding mode of the receptor with the metal ion as given in the diagram below. Similarly, the host-guest chemistry between receptor 4 and the Fe^{3+} ion was quickly identified by a proton NMR study (Fig. 11(b)). Here also H_a and H_b protons were downfield-shifted by 0.04 and 0.14 ppm, respectively, with no changes in the chemical shifts of the other protons, even in the presence of more than 1 equiv. of Fe^{3+} ion in the solution of receptor 4. Thus, the ^1H NMR titration study concludes the binding site for Hg^{2+} and Fe^{3+} to be a nitrogen atom of the triazole ring and the oxygen atom of the OCH_2 group linked to the fluorescein moiety.

4. Conclusion

In conclusion, a novel fluorescein-based ratiometric fluorescent chemosensor with a ferrocene backbone has been successfully designed

and synthesized. It shows good selectivity towards Fe^{3+} and Hg^{2+} ions via multiple channels with a very low limit of detection, a high binding constant and “zero-wait” response time. The present probe exhibits a negative solvatochromism in protic solvents, which may be due to a hydrogen bonding interaction between the fluorescein moiety and the corresponding polar solvent. Further, the present probe exhibits an anodic shift of $\Delta E_{1/2} = 33$ mV and 31 mV upon binding Hg^{2+} and Fe^{3+} ions, respectively. To the best of our knowledge, our probe is the 1st example of ferrocene based-fluorescein derivative for the detection of Hg^{2+} and Fe^{3+} ions simultaneously via ratiometric fluorescence and electrochemical studies. Thus, in real-time detection based on the promising ratiometric feature, the protocol described in this article opens a new entry for the design of fluorescent and electrochemical sensors for an easy and reliable detection of metal ions in real environmental samples.

Acknowledgment

Generous support of the Department of Science and Technology, DST, New Delhi for Inspire Faculty fellowship (IFA/14/CH-161) is gratefully acknowledged.

Appendix A. Supplementary data

Supplementary data to this article can be found online at <https://doi.org/10.1016/j.ica.2019.119097>.

References

- [1] A.R. Lippert, E.J. New, C.J. Chang, Reaction-based fluorescent probes for selective imaging of hydrogen sulfide in living cells, *J. Am. Chem. Soc.* 133 (2011) 10078–10080.
- [2] H. Kobayashi, M. Ogawa, R. Alford, P.L. Choyke, Y. Urano, New strategies for fluorescent probe design in medical diagnostic imaging, *Chem. Rev.* 110 (2010) 2620–2640.
- [3] H. Peng, Y. Cheng, C. Dai, A.L. King, B.L. Predmore, D.J. Lefer, B.A. Wang, Fluorescent probe for fast and quantitative detection of hydrogen sulfide in blood, *Angew. Chem. Int. Ed.* 50 (2011) 9672–9675.
- [4] L. Cui, Z. Peng, C. Ji, J. Huang, D. Huang, J. Ma, S. Zhang, X. Qian, Y. Xu, Hydrazine detection in the gas state and aqueous solution based on the Gabriel mechanism and its imaging in living cells, *Chem. Commun.* 50 (2014) 1485–1487.
- [5] M.H. Lee, B. Yoon, J.S. Kim, J.L. Sessler, Naphthalimide trifluoroacetyl acetate: a hydrazine-selective chemodosimetric sensor, *Chem. Sci.* 4 (2013) 4121–4126.
- [6] L. Cui, C. Ji, Z. Peng, L. Zhong, C. Zhou, L. Yan, S. Qu, S. Zhang, C. Huang, X. Qian, Y. Xu, Unique tri-output optical probe for specific and ultrasensitive detection of hydrazine, *Anal. Chem.* 86 (2014) 4611–4617.
- [7] Y. Sun, D. Zhao, S. Fan, L. Duan, A 4-hydroxynaphthalimide-derived ratiometric fluorescent probe for hydrazine and its *in vivo* applications, *Sens. Actuators, B* 208 (2015) 512–517.
- [8] B. Zhu, C. Gao, Y.C. Zhao, Y. Li, Q. Wei, Z. Ma, B. Du, X. Zhang, A 4-hydroxynaphthalimide-derived ratiometric fluorescent chemodosimeter for imaging palladium in living cells, *Chem. Commun.* 47 (2011) 8656–8658.
- [9] M.H. Lee, J.S. Kim, J.L. Sessler, Small molecule-based ratiometric fluorescence probes for cations, anions, and biomolecules, *Chem. Soc. Rev.* 44 (2015) 4185–4191.
- [10] W. Yin, H. Zhu, R.A. Wang, Sensitive and selective fluorescence probe based fluorescein for detection of hypochlorous acid and its application for biological imaging, *Dyes Pigments* 107 (2014) 127–132.
- [11] Y. Zhou, J.-Y. Li, K.-H. Chu, K. Liu, C. Yao, J.-Y. Li, Fluorescence turn-on detection of hypochlorous acid via HOCl-promoted dihydro fluorescein-ether oxidation and its application *in vivo*, *Chem. Commun.* 48 (2012) 4677–4679.
- [12] X.Q. Xiong, F.L. Song, G.W. Chen, W. Sun, J.Y. Wang, P. Gao, Construction of long-wavelength fluorescein analogues and their application as fluorescent probes, *Chem. Eur. J.* 19 (2013) 6538–6545.
- [13] J.M. An, M.H. Yan, Z.Y. Yang, T.R. Li, Q.X. Zhou, A turn-on fluorescent sensor for Zn(II) based on fluorescein-coumarin conjugate, *Dyes Pigments* 99 (2013) 1–5.
- [14] H.J. Kim, J.E. Park, M.G. Choi, S. Ahn, S.K. Chang, Selective chromogenic and fluorogenic signalling of Hg^{2+} ions using a fluorescein-coumarin conjugate, *Dyes Pigments* 84 (2010) 54–58.
- [15] Y. Duan, M. Liu, W. Sun, M. Wang, S. Liu, Q. Li, Recent progress on synthesis of fluorescein probes, *Mini Rev. Org. Chem.* 6 (2009) 35–43.
- [16] H.N. Kim, Z.Q. Guo, W.H. Zhu, J. Yoon, H. Tian, Recent progress on polymer-based fluorescent and colorimetric chemosensors, *Chem. Soc. Rev.* 40 (2011) 79–93.
- [17] R.F. Murphy, C.R. Powers, J. Cantor, Endosome pH measured in single cells by dual fluorescence flow cytometry: rapid acidification of insulin to pH 6, *Cell. Biol.* 98 (1984) 1757–1762.
- [18] M.J. Geisow, Fluorescein conjugates as indicators of subcellular pH: A critical evaluation, *Exp. Cell Res.* 150 (1984) 29–35.
- [19] D.F. Babcock, D.R. Pfeiffer, Independent elevation of cytosolic $[\text{Ca}^{2+}]$ and pH of mammalian sperm by voltage-dependent and pH-sensitive mechanisms, *J. Biol. Chem.* 262 (1987) 15041–15047.
- [20] N. Klonis, A.H.A. Clayton, E.W. Voss Jr, W.H. Sawyer, Spectral properties of fluorescein in solvent-water mixtures: applications as a probe of hydrogen bonding environments in biological systems, *Photochem. Photobiol.* 67 (1998) 500–510.
- [21] A.G. Miller, Ethylated fluoresceins: Assay of cytochrome P-450 activity and application to measurements in single cells by flow cytometry, *Anal. Biochem.* 133 (1983) 46–57.
- [22] S.R. Bhatta, V. Bhemireddy, G. Vijaykumar, A. Thakur, Triazole appended mono and 1,1'-di-substituted ferrocene-naphthalene conjugates: Highly selective and sensitive multi-responsive probes for Hg(II), *Sens. Actuators, B* 240 (2017) 640–650.
- [23] A. Tasleem, M. Azam, K. Siddiqui, A. Ali, I. Choi, Q. Mohd, R. Haq, Heavy metals and human health: mechanistic insight into toxicity and counter defense system of antioxidants, *Int. J. Mol. Sci.* 16 (2015) 29592–29630.
- [24] M. Ozdemir, A rhodamine-based colorimetric and fluorescent probe for dual sensing of Cu^{2+} and Hg^{2+} ions, *J. Photochem. Photobiol.* 318 (2016) 7–13.
- [25] M. Kaur, Y.H. Ahn, K. Choi, M.J. Cho, D.H. Choi, A bifunctional colorimetric fluorescent probe for Hg^{2+} and Cu^{2+} based on a carbazole-pyrimidine conjugate: chromogenic and fluorogenic recognition on TLC, silica-gel and filter paper, *Org. Biomol. Chem.* 13 (2015) 7149–7153.
- [26] Y. Gao, C. Zhang, S. Peng, H. Chen, A fluorescent and colorimetric probe enables simultaneous differential detection of Hg^{2+} and Cu^{2+} by two different mechanisms, *Sens. Actuators, B* 238 (2017) 455–461.
- [27] M. Li, Y. Sun, L. Dong, Q. Feng, H. Xu, S. Zang, T.C.W. Mak, Colorimetric recognition of Cu^{2+} and fluorescent detection of Hg^{2+} in aqueous media by a dual chemosensor derived from rhodamine B dye with a NS_2 receptor, *Sens. Actuators, B* 226 (2016) 332–341.
- [28] L. Liang, C. Liu, X. Jiao, L. Zhao, X. Zeng, A highly selective and sensitive photo-induced electron transfer (PET) based HOCl fluorescent probe in water and its endogenous imaging in living cells, *Chem. Commun.* 52 (2016) 7982–7985.
- [29] Y. Liu, D. Yu, S. Ding, Q. Xiao, J. Guo, G. Feng, Rapid and ratiometric fluorescent detection of cysteine with high selectivity and sensitivity by a simple and readily available probe, *ACS Appl. Mater. Interfaces* 6 (2014) 17543–17550.
- [30] A. Kaur, J.L. Kolanowski, E.J. New, Reversible fluorescent probes for biological redox states, *Angew. Chem. Int. Ed.* 55 (2016) 1602–1613.
- [31] L. Yuan, W. Lin, K. Zheng, L. He, W. Huang, Far-red to near infrared analyte responsive fluorescent probes based on organic fluorophore platforms for fluorescence imaging, *Chem. Soc. Rev.* 42 (2013) 622–661.
- [32] M.J. Kotze, D.P. van Velden, S.J. van Rensburg, R. Erasmus, Pathogenic mechanisms underlying iron deficiency and iron overload: new insights for clinical application, *EJIFCC* 20 (2009) 108–123.
- [33] J.S. Perlmutter, L.W. Tempel, K.J. Black, D. Parkinson, R.D. Todd, MPTP induces dystonia and parkinsonism clues to the pathophysiology of dystonia, *Neurology* 49 (1997) 1432–1438.
- [34] C.-F. Wan, Y.-J. Chang, C.-Y. Chien, Y.-W. Sie, C.-H. Hu, A.-T. Wu, A new multifunctional Schiff base as a fluorescence sensor for Fe^{2+} and F^- ions, and a colorimetric sensor for Fe^{3+} , *J. Lumin.* 178 (2016) 115–120.
- [35] L. Chen, X. Tian, D. Xia, Y. Nie, L. Lu, C. Yang, Z. Zhou, Novel colorimetric method for simultaneous detection and identification of multimetal ions in water: sensitivity, selectivity, and recognition mechanism, *ACS Omega* 4 (2019) 5915–5922.
- [36] R.K. Pathak, J. Dessingou, V.K. Hinge, A.G. Thawari, S.K. Basu, C.P. Rao, Quinoline driven fluorescence turn on 1,3-Bis-calix[4]arene conjugate-based receptor to discriminate Fe^{3+} from Fe^{2+} , *Anal. Chem.* 85 (2013) 3707–3714.
- [37] G.J. Park, G.R. You, Y.W. Choi, C. Kim, A naked-eye chemosensor for simultaneous detection of iron and copper ions and its copper complex for colorimetric/fluorescent sensing of cyanide, *Sens. Actuators, B* 229 (2016) 257–271.
- [38] S.-K. Lee, Y.-S. Noh, K.-I. Son, D.-Y. Noh, Chromotropic ferrocenyl chalcone with two pyrenyl groups: solvatochromism and molecular chemosensor for Fe(III)/Fe(II) ions, *Inorg. Chem. Commun.* 13 (2010) 1343–1346.
- [39] Y.S. Kim, G.J. Park, J.J. Lee, S.Y. Lee, S.Y. Lee, C. Kim, Multiple target chemosensor: a fluorescent sensor for Zn(II) and Al(III) and a chromogenic sensor for Fe(II) and Fe(III), *RSC Adv.* 5 (2015) 11229–11239.
- [40] T.G. Jo, K.H. Bok, J. Han, M.H. Lim, C. Kim, Colorimetric detection of Fe^{3+} and Fe^{2+} and sequential fluorescent detection of Al^{3+} and pyrophosphate by an imidazole-based chemosensor in a near-perfect aqueous solution, *Dyes Pigments* 139 (2017) 136–147.
- [41] H. Kim, Y.J. Na, E.J. Song, K.B. Kim, J.M. Bae, C. Kim, A single colorimetric sensor for multiple target ions: the simultaneous detection of Fe^{2+} and Cu^{2+} in aqueous media, *RSC Adv.* 4 (2014) 22463–22469.
- [42] Z.-Q. Liang, C.-X. Wang, J.-X. Yang, H.-W. Gao, Y.-P. Tian, X.-T. Tao, M.-H. Jiang, A highly selective colorimetric chemosensor for detecting the respective amounts of iron (II) and iron (III) ions in water, *New J. Chem.* 31 (2007) 906–910.
- [43] S.R. Bhatta, V. Bhemireddy, G. Vijaykumar, S. Debnath, A. Thakur, An efficient molecular tool with ferrocene backbone: discriminating Fe^{3+} from Fe^{2+} in aqueous media, *Organometallics* 36 (2017) 2141–2152.
- [44] S. Sen, S. Sarkar, B. Chattopadhyay, A. Moirangthem, A. Basu, K. Dharad, P. Chattopadhyay, A ratiometric fluorescent chemosensor for iron: discrimination of Fe^{2+} and Fe^{3+} and living cell application, *Analyst* 137 (2012) 3335–3342.
- [45] Q. Mei, C. Jiang, G. Guan, K. Zhang, B. Liu, R. Liu, Z. Zhang, Fluorescent graphene oxide logic gates for discrimination of iron (3+) and iron (2+) in living cells by imaging, *Chem Commun.* 48 (2012) 7468–7470.
- [46] A. Han, X. Liu, G.D. Prestwich, L. Zang, Fluorescent sensor for Hg^{2+} detection in aqueous solution, *Sens. Actuators, B* 198 (2014) 274–277.

- [47] M. Vedamalai, D. Kedaria, R. Vasita, S. Moric, I. Gupta, Design and synthesis of BODIPY-clickate based Hg^{2+} sensors: the effect of triazole binding mode with Hg^{2+} on signal transduction, *Dalton Trans.* 45 (2016) 2700–2708.
- [48] X. Wu, Q. Niu, T. Li, A novel urea-based “turn-on” fluorescent sensor for detection of Fe^{3+}/F^{-} ions with high selectivity and sensitivity, *Sens. Actuators, B* 222 (2016) 714–720.
- [49] S. Zhang, Q. Niu, L. Lan, T. Li, Novel oligothiophene-phenylamine based Schiff base as a fluorescent chemosensor for the dual-channel detection of Hg^{2+} and Cu^{2+} with high sensitivity and selectivity, *Sens. Actuators, B* 240 (2017) 793–800.
- [50] Q. Niu, T. Sun, T. Li, Z. Guo, H. Pang, Highly sensitive and selective colorimetric/fluorescent probe with aggregation induced emission characteristics for multiple targets of copper, zinc and cyanide ions sensing and its practical application in water and food samples, *Sens. Actuators, B* 266 (2018) 730–743.
- [51] T. Sun, Q. Niu, T. Li, Z. Guo, H. Liu, A simple, reversible, colorimetric and water-soluble fluorescent chemosensor for the naked-eye detection of Cu^{2+} in ~100% aqueous media and application to real samples, *Spectrochim. Acta* 188 (2018) 411–417.
- [52] S. Zhang, T. Sun, D. Xiao, F. Yuan, T. Li, E. Wang, H. Liu, Q. Niu, A dual-responsive colorimetric and fluorescent chemosensor based on diketopyrrolopyrrole derivative for naked-eye detection of Fe^{3+} and its practical application, *Spectrochim. Acta* 189 (2018) 594–600.
- [53] T. Sun, Y. Li, Q. Niu, T. Li, Y. Liu, Highly selective and sensitive determination of Cu^{2+} in drink and water samples based on a 1,8-diaminonaphthalene derived fluorescent sensor, *Spectrochim. Acta* 195 (2018) 142–147.
- [54] Z. Guo, Q. Niu, T. Li, Highly sensitive oligothiophene-phenylamine-based dual-functional fluorescence “turn-on” sensor for rapid and simultaneous detection of Al^{3+} and Fe^{3+} in environment and food samples, *Spectrochim. Acta* 200 (2018) 76–84.
- [55] Z. Guo, Q. Niu, T. Li, T. Sun, H. Chi, A fast, highly selective and sensitive colorimetric and fluorescent sensor for Cu^{2+} and its application in real water and food samples, *Spectrochim. Acta* 213 (2019) 97–103.
- [56] L. Lan, Q. Niu, Z. Guo, H. Liu, T. Li, Highly sensitive and fast responsive “turn-on” fluorescent sensor for selectively sensing Fe^{3+} and Hg^{2+} in aqueous media based on an oligothiophene derivative and its application in real water samples, *Sens. Actuators, B* 244 (2017) 500–508.
- [57] B. Shen, Y. Qian, Building rhodamine-BODIPY fluorescent platform using click reaction: Naked-eye visible and multi-channel chemodosimeter for detection of Fe^{3+} and Hg^{2+} , *Sens. Actuators, B* 260 (2018) 666–675.
- [58] B. Shen, Y. Qian, Triphenylamine-BODIPY fluorescent dendron: Click synthesis and fluorometric chemodosimeter for Hg^{2+} , Fe^{3+} based on the C=N bond, *Chemistry Select* 2 (2017) 2406–2413.
- [59] H. Lv, Z. Ren, H. Liu, G. Zhang, H. He, X. Zhang, S. Wang, The turn-off fluorescent sensors based on thioether-linked bisbenzamide for Fe^{3+} and Hg^{2+} , *Tetrahedron* 74 (2018) 1668–1680.
- [60] M. Maniyazagan, C. Rameshwaran, R. Mariadasse, J. Jeyakanthan, T. Stalin, K. Premkumar, Premkumar Fluorescence sensor for Hg^{2+} and Fe^{3+} ions using 3,3-Dihydroxybenzidine: α -Cyclodextrin supramolecular complex: characterization, in-silico and cell imaging study, *Sens. Actuators, B* 242 (2017) 1227–1238.
- [61] F. Perez-Balderas, M. Ortega-Muñoz, J. Morales-Sanfrutos, F. Hernández-Mateo, F.G. Calvo-Flores, J.A. Calvo-Asín, J. Isac-García, F. Santoyo-González, Multivalent neo glycoconjugates by regiospecific cycloaddition of alkynes and azides using organic-soluble copper catalysts, *Org. Lett.* 5 (2003) 1951–1954.
- [62] J.M. Casas-Solvas, A. Vargas-Berenguel, L.F. Capitán-Vallvey, F. Santoyo-González, Convenient methods for the synthesis of ferrocene-carbohydrate conjugates, *Org. Lett.* 6 (2004) 3687–3690.
- [63] Y. Ruan, J. Xie, Unexpected highly selective fluorescence ‘turn-on’ and ratiometric detection of Hg^{2+} based on fluorescein platform, *Tetrahedron Lett.* 52 (2011) 5234–5237.
- [64] A. Barba-Bon, A.M. Costero, S. Gil, M. Parra, J. Soto, R. Martínez-Mañez, F. Sancenón, A new selective fluorogenic probe for trivalent cations, *Chem. Commun.* 48 (2012) 3000–3002.
- [65] A.C. Gonçalves, V. Pilla, E. Oliveira, S.M. Santos, J.L. Capelo, A.A. Dos Santos, C. Lodeiro, The interaction of Hg^{2+} and trivalent ions with two new fluorescein bio-inspired dual colorimetric/fluorimetric probes, *Dalton Trans.* 45 (2016) 9513–9522.
- [66] R.J. Radford, W. Chyan, S.J. Lippard, Peptide targeting of fluorescein-based sensors to discrete intracellular locales, *Chem. Sci.* 5 (2014) 4512–4516.
- [67] Z.-H. Fu, Y.-W. Wang, Y. Peng, Two fluorescein-based chemosensors for the fast detection of 2,4,6-trinitrophenol (TNP) in water, *Chem. Commun.* 53 (2017) 10524–10527.
- [68] X. Peng, Y. Xu, S. Sun, Y. Wu, J. Fan, A ratiometric fluorescent sensor for phosphates: Zn^{2+} -enhanced ICT and ligand competition, *Org. Biomol. Chem.* 5 (2007) 226–228.
- [69] M. Shyamal, P. Mazumdar, S. Maity, G.P. Sahoo, G. Salgado Morán, A. Misra, Pyrene scaffold as real-time fluorescent turn-on chemosensor for Selective detection of trace-level Al(III) and Its aggregation-induced emission enhancement, *J. Phys. Chem. A* 120 (2016) 210–220.
- [70] L. Wang, Y.-Q. Fan, X.-W. Guan, W.-J. Qu, Q. Lin, H. Yao, T.-B. Wei, Y.-M. Zhang, A novel naphthalimide-glutathione chemosensor for fluorescent detection of Fe^{3+} and Hg^{2+} in aqueous medium and its application, *Tetrahedron* 74 (2018) 4005–4012.
- [71] X. Liu, N. Li, M.-M. Xu, C. Jiang, J. Wang, G. Song, Y. Wang, Dual sensing performance of 1, 2-squaraine for the colorimetric detection of Fe^{3+} and Hg^{2+} ions, *Materials* 11 (2018) 1998–2014.
- [72] J. Liu, Y. Qian, A novel pyridylvinyl naphthalimide-rhodamine dye: Synthesis, naked-eye visible and ratiometric chemodosimeter for Hg^{2+}/Fe^{3+} , *J. Lumin.* 187 (2017) 33–39.
- [73] P. Kaur, D. Sareen, The synthesis and development of a dual-analyte colorimetric sensor: Simultaneous estimation of Hg^{2+} and Fe^{3+} , *Dyes Pigments* 88 (2011) 296–300.
- [74] A. Rai, A.K. Singh, A.K. Sonkar, A. Prakash, J.K. Roy, R. Nagarajan, L. Mishra, A smart switchable module for the detection of multiple ions via turn-on dual-optical readout and their cell imaging studies, *Dalton Trans.* 45 (2016) 8272–8277.
- [75] X. Zhou, X. Wub, J. Yoon, A dual FRET based fluorescent probe as a multiple logic system, *Chem. Commun.* 51 (2015) 111–113.
- [76] J. Liu, Y. Qian, A novel naphthalimide-rhodamine dye: Intramolecular fluorescence resonance energy transfer and ratiometric chemodosimeter for Hg^{2+} and Fe^{3+} , *Dyes Pigments* 136 (2017) 782–790.
- [77] X. Cao, N. Zhao, A. Gao, Q. Ding, Y. Li, X. Chang, Terminal molecular isomer-effect on supramolecular self-assembly system based on naphthalimide derivative and its sensing application for mercury(II) and iron(III) ions, *Langmuir* 34 (2018) 7404–7415.
- [78] T. Sun, Q. Niu, Y. Li, T. Li, H. Liu, Novel oligothiophene-based dual-mode chemosensor: “Naked-Eye” colorimetric recognition of Hg^{2+} and sequential off-on fluorescence detection of Fe^{3+} and Hg^{2+} in aqueous media and its application in practical samples, *Sens. Actuators, B* 248 (2017) 24–34.
- [79] A.I. Said, N.I. Georgiev, V.B. Bojinov, Synthesis of a single 1,8-naphthalimide fluorophore as a molecular logic lab for simultaneously detecting of Fe^{3+} , Hg^{2+} and Cu^{2+} , *Spectrochim. Acta* 196 (2018) 76–82.
- [80] L. Lan, Q. Niu, T. Li, A highly selective colorimetric and ratiometric fluorescent probe for instantaneous sensing of Hg^{2+} in water, soil and seafood and its application on test strips, *Anal. Chim. Acta* 1023 (2018) 105–114.
- [81] Y. Li, Q. Niu, T. Wei, T. Li, Novel thiophene-based colorimetric and fluorescent turn-on sensor for highly sensitive and selective simultaneous detection of Al^{3+} and Zn^{2+} in water and food samples and its application in bioimaging, *Anal. Chim. Acta* 1049 (2019) 196–212.
- [82] Z. Zuo, X. Song, D. Guo, Z. Guob, Q. Niu, A dual responsive colorimetric/fluorescent turn-on sensor for highly selective, sensitive and fast detection of Fe^{3+} ions and its applications, *J. Photochem. Photobiol. A: Chem.* 382 (2019) 111876–111883.
- [83] S. Kim, M. Fujitsuka, T. Majima, Photochemistry of Singlet Oxygen Sensor Green, *J. Phys. Chem. B* 117 (2013) 13985–13992.
- [84] F. Naderi, A. Farajtabar, Solvatochromism of fluorescein in aqueous aprotic solvents, *J. Mol. Liq.* 221 (2016) 102–107.
- [85] A. Mazzoli, B. Carloti, C. Bonaccorso, C.G. Fortuna, U. Mazzucato, G. Miolo, A. Spalletti, Photochemistry and DNA-affinity of some pyrimidine-substituted styryl-azinium iodides, *Photochem. Photobiol. Sci.* 10 (2011) 1830–1836.
- [86] B. Carloti, A. Cesaretti, C.G. Fortuna, A. Spalletti, F. Elisei, Experimental evidence of dual emission in a negatively solvatochromic push-pull pyridinium derivative, *Phys. Chem. Chem. Phys.* 17 (2015) 1877–1882.
- [87] B. Carloti, G. Consiglio, F. Elisei, C.G. Fortuna, U. Mazzucato, A. Spalletti, Intramolecular charge transfer of push-pull pyridinium salts in the singlet manifold, *J. Phys. Chem. A* 118 (2014) 3580–3592.
- [88] H.M. Rageh, M.M. Abou-Krishna, A.M. Abo-bakr, M. Abd-Elasbour, Electrochemical behavior and the detection limit of ascorbic acid on a Pt modified electrode, *Int. J. Electrochem. Sci.* 10 (2015) 4105–4115.